

Giant resonances near the split band edges of two-dimensional photonic crystals

Heeso Noh,¹ Jin-Kyu Yang,¹ Ilya Vitebskiy,² Alex Figotin,² and Hui Cao^{1,3}

¹*Department of Applied Physics, Yale University, New Haven, Connecticut 06520, USA*

²*Department of Mathematics, University of California at Irvine, Irvine, California 92697, USA*

³*Department of Physics, Yale University, New Haven, Connecticut 06520, USA*

(Received 15 May 2010; published 2 July 2010)

We conduct a numerical study on the giant optical resonances near the split photonic band edges of two-dimensional square lattices. Their quality factors are 1 order of magnitude higher than those near the regular band edges. Such enhancement results from the efficient interference of multiple Bloch waves, which minimizes light leakage from the periodic pattern of finite size. The variation of the quality factor with the pattern size is nonmonotonic for the split band edge resonance, leading to an optimal size for the maximal quality factor.

DOI: [10.1103/PhysRevA.82.013801](https://doi.org/10.1103/PhysRevA.82.013801)

PACS number(s): 42.70.Qs, 41.20.Jb

I. INTRODUCTION

Photonic crystals (PCs) have the potential for full control of light propagation and localization [1–4]. One attractive feature of PCs is the anomalous dispersion of photonic bands [5–7]. Near a photonic band edge (BE), the derivative of frequency ω to the Bloch wave vector k approaches zero, and the group velocity is greatly reduced [8–11]. The slow light can drastically enhance light-matter interactions, for example, light amplification and nonlinear wave mixing, thus having important applications to lasers, optical modulators, and switches [2,3,12,13].

Unlike the transmission resonance of a finite-sized PC, the quasimode has a complex frequency $\omega = \omega_r + i\omega_i$. The real part ω_r represents the frequency and the imaginary part the decay rate from light leakage through the PC boundaries. The quality (Q) factor, defined as the ratio of the energy stored in the PC to the energy being lost in one cycle, is equal to $Q = \omega_r/2\omega_i$. The Q factor of a BE mode in a finite-sized PC depends on the closeness of its frequency ω to the BE frequency ω_0 at which the group velocity vanishes. Usually ω is not equal to ω_0 because of the quantization of k . For example, in a one-dimensional (1-D) PC made of isotropic media, the BEs are located at the center or the boundary of the first Brillouin zone (BZ), where the Bloch wave vector $k_0 = 0$ or $\pm\pi/a$ (a is the lattice constant). The first band edge mode, the one closest to a BE in frequency, has $k_1 = k_0 \pm \pi/Na$, where N is the number of unit cells and Na is the total length of PC. At a regular band edge (RBE), the frequency of the first BE mode is $\omega_1 = \omega_0 + \alpha(k_1 - k_0)^2 = \omega_0 + \alpha(\pi/Na)^2$. Since v_g is nonzero at ω_1 , the RBE resonance has a finite lifetime or Q factor. The larger the N , the closer ω_1 to ω_0 , and the higher the Q . At a degenerate band edge (DBE), the dispersion curve, $\omega = \omega_0 + \beta(k - k_0)^4$, is flatter than that at a RBE (Fig. 1). The frequency ω_1 of the first BE mode can be much closer to ω_0 for the same N or k_1 [14,15]. Thus the DBE resonance may have significantly smaller v_g and higher Q than the RBE resonance. Instead of pushing ω_1 closer to ω_0 by increasing N , an alternative way of enhancing Q is bringing a stationary point (where $d\omega/dk = 0$) to $\pm k_1$ with a split band edge (SBE). It has been shown that a DBE can split into two RBEs in a 1-D periodic structure made of anisotropic materials [16,17]. This band edge configuration is referred to as the split band edge (Fig. 1). The dispersion relation is $\omega = \omega_0 + \alpha(k - k_0)^2 +$

$\beta(k - k_0)^4$, where $\alpha/\beta < 0$. As plotted schematically in Fig. 1, $v_g = 0$ at $k = k_0, \pm k_b$. k_b deviates from k_0 and may coincide with k_1 for an appropriate choice of N , leading to a vanishing v_g for the SBE resonance. This naive argument suggests the SBE resonance be much stronger than the RBE and DBE resonances. As demonstrated in the microwave experiment, the Q factor of a SBE resonance even exceeds that of a localized defect resonance in a 1-D anisotropic PC with $N = 16$ [17].

So far, most studies on the DBE and SBE resonances, both theoretical and experimental, have been conducted on 1-D PCs [14–35]. The Bloch dispersion relation of a periodic layered structure (a 1-D PC) can display a DBE or a SBE only if some of the layers are made of anisotropic materials with strong linear birefringence and misaligned optical axes [14,15]. At optical frequencies, such materials are not readily available. On the other hand, there are no fundamental restrictions on the existence of a DBE or a SBE in PCs with 2-D and 3-D periodicity. Such PCs can be made of any transparent optical materials, which provides a big practical advantage.

In this article, we have performed numerical calculations in search of the DBE and SBE resonances in 2-D PCs of realistic parameters [e.g., using the refractive index of Gallium Arsenide (GaAs) or silicon]. For the square lattices of air holes in dielectric media, we find the SBE resonances but not the DBE resonances. Their Q factors are over 1 order of magnitude higher than those of the RBE resonances in the same structures. We provide a qualitative explanation for such high Q in terms of interference of multiple Bloch waves. The article is organized as follows. Section II shows the SBE resonance in an ideal 2-D square lattice of infinitely long air cylinders in a dielectric medium. In Sec. III, we consider a more realistic 2-D structure, a PC slab of finite thickness, and find again the SBE resonance. Section IV is the conclusion.

II. 2-D SQUARE LATTICE

We first search for the SBE resonance in a 2-D square lattice of air cylinders in a dielectric medium. Let a be the lattice constant and r the radius of air cylinders. We consider the transverse electric (TE) polarization, namely, the magnetic field is parallel to the cylinder axis. Figure 2(a) shows the first and second photonic bands calculated with the plane wave

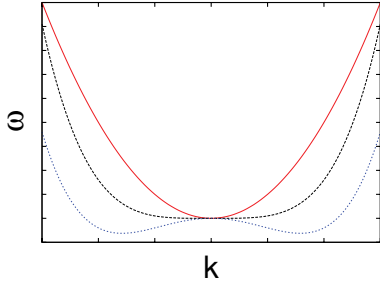


FIG. 1. (Color online) Dispersion curves at the RBE (red solid line), DBE (black dashed line), and SBE (blue dotted line).

expansion method [36]. The refractive index of the dielectric host is $n = 3.44$, and $r/a = 0.4$. In the Γ - M direction, the second band exhibits a SBE at the M point, as seen clearly in Fig. 2(b). The dispersion curve around the M point can be well fit by $(\omega - \omega_0)a/2\pi c = \alpha(ka)^2 + \beta(ka)^4$, with $\omega_0 a/2\pi c = 0.302$, $\alpha = -0.123$, and $\beta = 8.43$. Since $\alpha/\beta < 0$ and $|\alpha/\beta| = 0.01 \ll 1$, the conditions for the realization of high- Q SBE resonance are met [16]. We calculate the resonances in 2-D PCs of finite size using a commercial program (COMSOL) based on the finite element method. The boundaries are parallel to the Γ - M directions. Cartesian coordinates are set up [Fig. 3(a)] with the x and y axes along the Γ - M directions and the z axis parallel to the air cylinders. The 2-D pattern is symmetric with respect to the x and y axes. The lateral dimension is $L = (2N - 1)a/\sqrt{2}$, where N is an integer. The total number of unit cells is $N^2 + (N - 1)^2$. Owing to light escape through the boundaries of the periodic structure, the resonances have complex eigenfrequencies $\tilde{\omega}$, with the imaginary parts inversely proportional to the lifetimes.

Figure 3(a) shows the spatial profile of the highest Q resonance in the vicinity of SBE for $N = 15$. The magnetic field is parallel to the z axis and the electric field to the xy plane. The spatial distribution H_z is symmetric with respect to the x and y axes. The envelope of electric field intensity $|E_x|^2 + |E_y|^2$ along the x axis or y axis has double maxima [Fig. 3(b)]. Figure 4 plots the normalized frequency and Q

factor of this resonance as a function of N . While the frequency changes slightly with N , the Q factor exhibits a more dramatic variation. As N increases from 12 to 15, Q is enhanced by nearly 1 order of magnitude. A further increase of N from 15 to 17 results in a rapid drop of Q . This behavior is very different from the monotonic increase of Q with N for the RBE or DBE resonance. The maximal Q value is $\sim 17,000$, about 16 times higher than that of the RBE resonance at the first band edge of $\omega a/2\pi c = 0.26$.

Although the giant resonance shown in Fig. 3 is related to the SBE, its frequency ω_s is not equal to that of a stationary point. As shown in Fig. 5(a), there are three stationary points around the SBE: one at the M point with $k = k_0$ and $\omega = \omega_0$ and the other two at $k = k_0 \pm k_b$ and $\omega = \omega_b$. ω_s is between ω_0 and ω_b , $\omega_b < \omega_s < \omega_0$. The dispersion curve gives $k = k_0 \pm k_{s1}, k_0 \pm k_{s2}$ at $\omega = \omega_s$. For $N = 15$, $k_{s1} = k_1 = \pi/L$ and $k_{s2} = 3k_1$. The SBE resonance contains two pairs of counterpropagating Bloch waves in the x direction (Γ - M direction), with $k_x = k_0 \pm k_1, k_0 \pm 3k_1$, and another two pairs in the y direction (also Γ - M direction), with $k_y = k_0 \pm k_1, k_0 \pm 3k_1$. The destructive interference among the multiple Bloch waves near the boundaries of the PC greatly reduces light leakage, thus enhancing the lifetime or Q factor. This effect is stronger than that for a RBE resonance which has only one pair of counterpropagating Bloch waves in the x (or y) direction to interfere. Hence the envelope of field intensity for a SBE resonance has smaller tails at the boundaries than that of a RBE resonance, as seen in Fig. 3(b). When N is larger or smaller than 15, k_{s2} deviates from $3k_{s1}$. Since k must satisfy the quantization condition $k_{x,y} - k_0 = \pm k_1, \pm 2k_1, \pm 3k_1, \dots$, $\omega_{s1} = \omega(k_{x,y} = k_0 \pm k_1)$ is no longer equal to $\omega_{s2} = \omega(k_{x,y} = k_0 \pm 3k_1)$. The two counterpropagating Bloch waves with $k_{x(y)} = k_0 \pm k_1$ are frequency detuned from those of $k_{x(y)} = k_0 \pm 3k_1$. Their interaction is weakened, leading to a reduction in Q factor. For confirmation, we qualitatively reconstruct the envelope function for the SBE resonance by mixing waves with $\pm k$ and $\pm 3k$. The value of k_0 is set to 0 as it does not affect the envelope function. Figure 5(b) plots the spatial distribution of a function $f(x, y) = [\cos(kx) - 0.2 \cos(3kx)][\cos(ky) - 0.2 \cos(3ky)]$. It resembles the spatial

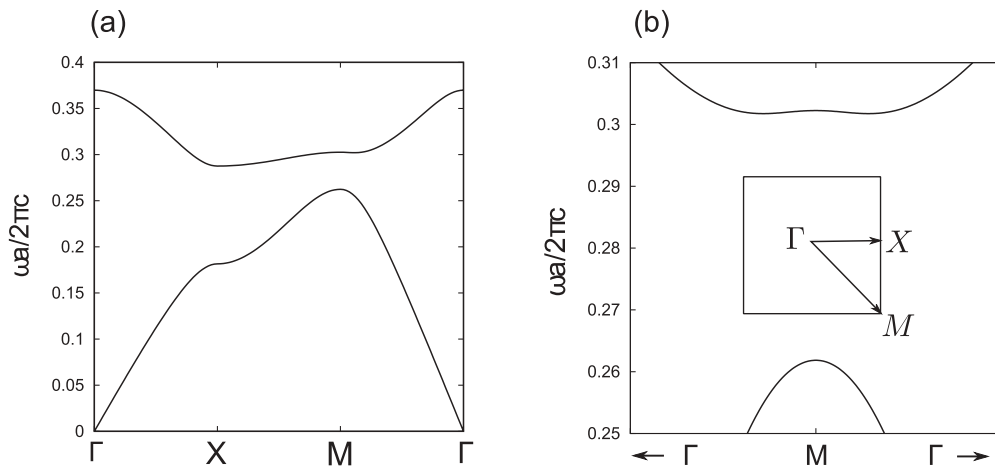


FIG. 2. (a) Photonic bands of TE polarization in a 2-D square lattice of air cylinders in a dielectric medium; $n = 3.44$ and $r/a = 0.4$. (b) Expanded view of the photonic bands near the M point and along the Γ - M direction. Inset shows the first Brillouin zone of the square lattice.

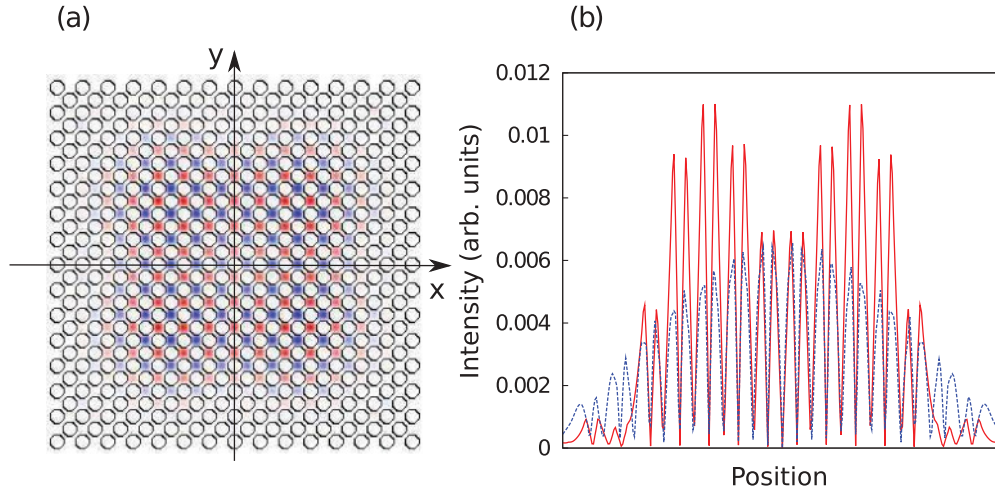


FIG. 3. (Color online) (a) Spatial distribution of the magnetic field for the SBE resonance at $\omega a/2\pi c = 0.305$, overlaid on the structure of $N = 15$. (b) Electric field intensity along the x axis (or y axis) for the SBE resonance (red solid line) and the RBE (blue dashed line). The electric field intensity is normalized such that its integration over the entire pattern area is equal to unity.

profile of the SBE resonance shown in Fig. 3(a). Therefore the high Q of the SBE resonance is caused not by the vanishing v_g at the stationary point ($\omega = \omega_b$) but by the interference of multiple Bloch waves with the same frequency. Note that k_{s2} cannot be equal to $2k_1$ when $k_{s1} = k_1$. The envelope of a standing wave formed by two counterpropagating Bloch modes with $k_{x(y)} = k_0 \pm k$ has an even symmetry with respect to the $x(y)$ axis (Fig. 2), while that with $k_{x(y)} = k_0 \pm 2k$ has an odd symmetry. Hence they cannot couple to form a SBE resonance.

Let us remark that the previous consideration is based on the assumption that the quasimodes are superpositions of propagating Bloch waves. In close vicinity of a SBE, this may not be the case because of possible contributions of the evanescent Bloch waves. According to [14,15], the evanescent contribution can be appreciable if the shape of the SBE is very close to a DBE. Hence a quantitative explanation beyond

the scope of this article shall take into account the evanescent waves.

III. PHOTONIC CRYSTAL SLAB

The preceding studies are performed on ideal 2-D PCs with infinitely long cylinders. Experimentally, the cylinders always have finite length. A 2-D periodic structure having a finite thickness in the third dimension is referred to as a photonic crystal slab. In this section, we study the SBE resonances in the PC slabs.

We consider a 2-D square lattice of air holes in a dielectric slab. The refractive index of the dielectric material is 3.45, similar to that of GaAs or Si. The slab has a thickness t and is surrounded by air from above and below. Light is confined to the plane of the slab via index guiding. Figure 6(a) shows the guided photonic bands of TE polarization in a PC slab with $r/a = 0.4$ and $t/a = 0.61$. The shaded areas represent the light cones. The second band has a SBE at the M point ($M2$), similar to an ideal 2-D PC. The dispersion curve can be fit by $(\omega - \omega_0)a/2\pi c = \alpha(ka)^2 + \beta(ka)^4$, with $\omega_0 a/2\pi c = 0.351$, $\alpha = -0.0942$, and $\beta = 7.66$. The absolute values of α and β are slightly smaller than those of the ideal 2-D PC with the same n and r/a , indicating that the dispersion curve is a little flatter for the PC slab.

Next we calculate the SBE resonances in PC slabs of different N using the 3-D FDTD program. Light may escape vertically through the top and bottom interfaces of the slab into air and laterally through the boundary of the periodic pattern to the unpatterned part of the slab. The vertical leakage rate is characterized by the out-of-plane energy loss per optical cycle Q_{\perp}^{-1} , the lateral by Q_{\parallel}^{-1} . The total loss rate is described by $Q_{tot}^{-1} = Q_{\perp}^{-1} + Q_{\parallel}^{-1}$. Figure 6(b) shows the spatial distribution of electric field intensity for the TE-polarized SBE resonance with $N = 15$. Its $Q_{tot} \simeq 33,000$, and $Q_{\parallel}/Q_{\perp} \sim 0.3$. Since the in-plane leakage is three times larger than the out-of-plane leakage, it dominates the total loss. The nonmonotonic variation of Q_{\parallel} with N results in a local maximum of Q_{tot} at $N = 15$ (Fig. 7). Despite the additional loss in the vertical

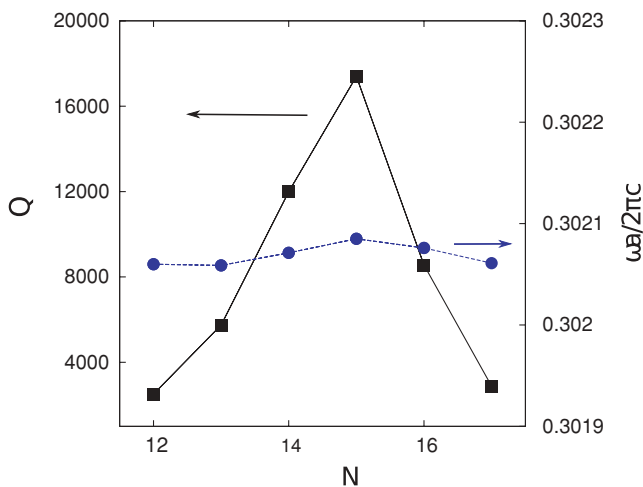


FIG. 4. (Color online) Q factor and normalized frequency of the SBE resonance in a 2-D square lattice as a function of the pattern size N .

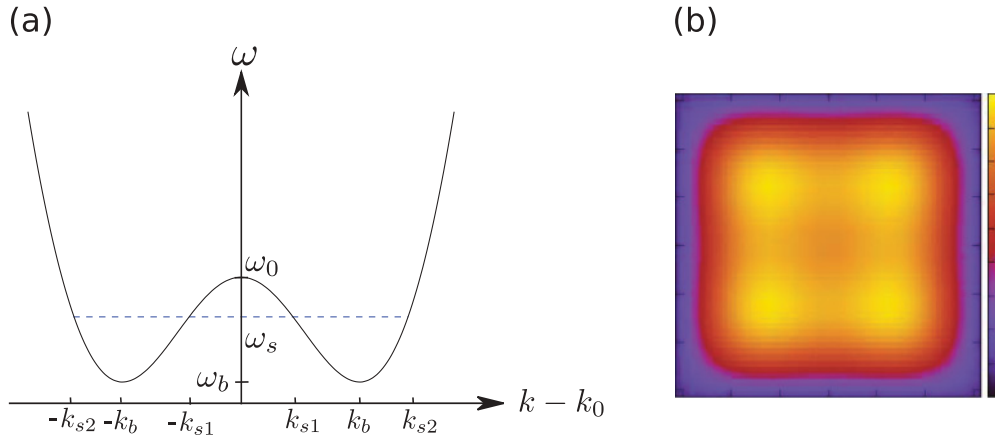


FIG. 5. (Color online) (a) Schematic diagram showing that the SBE resonance consists of Bloch waves with $k = k_0 \pm k_{s1}, k_0 \pm k_{s2}$. The frequency ω_s of the SBE resonance is between ω_0 and ω_b , where $d\omega/dk = 0$. (b) Reconstructed envelope function of the SBE mode based on the $3k_1 = k_3$ relation.

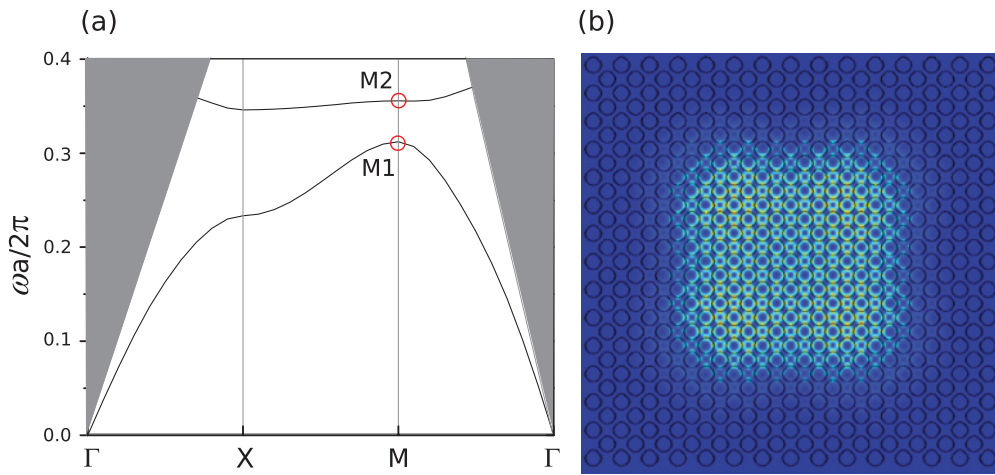


FIG. 6. (Color online) (a) Guided TE bands in a PC slab of square lattice; $r/a = 0.4$, $n = 3.45$, and $t/a = 0.61$. (b) Spatial distribution of electric field intensity of the SBE resonance at $M2$ point; $N = 15$.

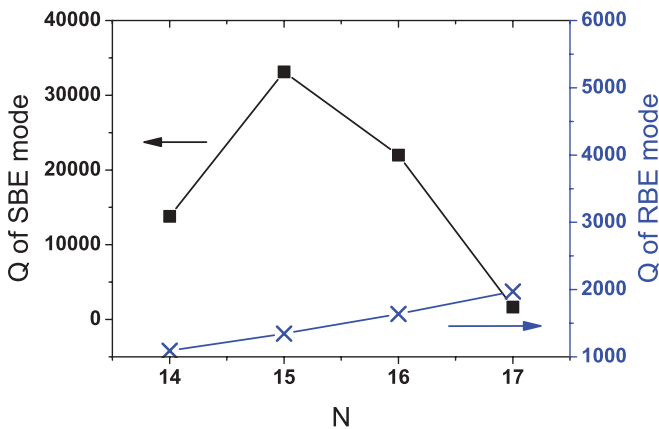


FIG. 7. (Color online) Q factors of the SBE resonance (squares) and the RBE resonance (crosses) as a function of the pattern size N ; $r/a = 0.4$, $n = 3.45$, and $t/a = 0.61$.

direction, Q_{tot} of the SBE resonance in the PC slab is about a factor of 2 larger than that in the 2-D PC with the same N and n . This is because Q_{tot} is determined mostly by $Q_{||}$, which is larger than that of the 2-D PC because of the flatter dispersion curve near the SBE in the PC slab [37]. Figure 7 also plots Q_{tot} of the RBE resonance at the $M1$ point [Fig. 6(a)]. It increases monotonically with N , as expected. At $N = 15$, the Q_{tot} of the SBE resonance is about 25 times larger than that of the RBE resonance.

IV. CONCLUSION

We have found the SBE resonances in 2-D PCs and PC slabs. Their Q values are over an order of magnitude higher than those of the RBE resonances in the same structure. Such high Q factors are attributed to the efficient interference of multiple Bloch waves, which minimize light leakage from the periodic pattern of finite size. The variation of the Q value with the pattern size is nonmonotonic for the SBE resonance, leading to an optimal size for the maximal Q .

The SBE resonances offer exciting opportunities for the application of on-chip lasers and optical sensors. The SBE

laser may combine the advantages of the PC defect mode laser and the regular band edge laser to obtain simultaneously low lasing threshold and strong emission intensity. On one hand, the SBE modes have much higher Q factor than the RBE modes, and thus the lasing threshold is significantly lower. On the other hand, they have much larger spatial

overlap with the gain materials than the defect modes so that the laser emission can be much stronger. Moreover, the SBE resonances may greatly enhance the sensitivity of label-free optical sensors because they simultaneously have narrow line width and high field intensity in the detection region.

-
- [1] J. D. Joannopoulos, S. Johnson, J. Winn, and R. Meade, *Photonic Crystals: Molding the Flow of Light* (Princeton University Press, Princeton, 2008).
- [2] S. Noda and T. Baba (eds.), *Roadmap on Photonic Crystals* (Kluwer Academic, Dordrecht, 2003).
- [3] C. M. Soukoulis (ed.), *Photonic Crystals and Light Localization in the 21st Century* (Kluwer Academic, Norwell, 2001).
- [4] S. G. Johnson, Ph.D. thesis, MIT, 2001.
- [5] A. Figotin and I. Vitebskiy, *Waves Random Complex Media* **16**, 293 (2006).
- [6] T. Baba, *Nat. Photon.* **2**, 465 (2008).
- [7] L. H. Frandsen, A. V. Lavrinenko, J. Fage-Pedersen, and P. I. Borel, *Opt. Express* **14**, 9444 (2006).
- [8] J. H. Chu, O. Voskoboinikov, and C. P. Lee, *Microelectron. J.* **36**, 282 (2005).
- [9] T. F. Krauss, *J. Phys. D* **40**, 2666 (2007).
- [10] D. A. B. Miller, *Phys. Rev. Lett.* **99**, 203903 (2007).
- [11] J. G. Pedersen, S. Xiao, and N. A. Mortensen, *Phys. Rev. B* **78**, 153101 (2008).
- [12] Y. Hamachi, S. Kubo, and T. Baba, *Opt. Lett.* **34**, 1072 (2009).
- [13] R. Iliew, C. Etrich, T. Pertsch, and F. Lederer, *Phys. Rev. B* **77**, 115124 (2008).
- [14] A. Figotin and I. Vitebskiy, *Phys. Rev. E* **74**, 066613 (2006).
- [15] A. Figotin and I. Vitebskiy, *Phys. Rev. E* **72**, 036619 (2005).
- [16] A. Figotin and I. Vitebskiy, *Phys. Rev. A* **76**, 053839 (2007).
- [17] A. A. Chabanov, *Phys. Rev. A* **77**, 033811 (2008).
- [18] K. Y. Jung and F. L. Teixeira, *Phys. Rev. B* **77**, 125108 (2008).
- [19] K. Y. Jung and F. L. Teixeira, *Phys. Rev. A* **78**, 043826 (2008).
- [20] R. A. Chilton, K. Y. Jung, R. Lee, and F. L. Teixeira, *IEEE Trans. Microw. Theor. Tech.* **55**, 2631 (2007).
- [21] C. Locker, K. Sertel, and J. L. Volakis, *IEEE Microw. Wireless Compon. Lett.* **16**, 642 (2006).
- [22] G. Mumcu, K. Sertel, and J. L. Volakis, *IEEE Trans. Antennas Propag.* **57**, 1618 (2009).
- [23] G. Mumcu, K. Sertel, J. L. Volakis, I. Vitebskiy, and A. Figotin, *IEEE Trans. Antennas Propag.* **53**, 4026 (2005).
- [24] M. B. Stephanson, K. Sertel, and J. L. Volakis, *IEEE Microw. Wireless Compon. Lett.* **18**, 305 (2008).
- [25] I. Vitebskiy and A. Figotin, in *Magnetolectric Interaction Phenomena in Crystals*, edited by M. Fiebig, V. V. Ereminenko, and I. E. Chupis (Kluwer Academic, Dordrecht, 2004), pp. 291–301.
- [26] J. L. Volakis, G. Mumcu, and K. Sertel, *IEICE Trans. Comm. E* **B 90**, 2203 (2007).
- [27] J. L. Volakis, G. Mumcu, K. Sertel, C. C. Chen, M. Lee, B. Kramer, D. Psychoudakis, and G. Kiziltas, *IEEE Trans. Antennas Propag.* **48**, 12 (2006).
- [28] J. L. Volakis, K. Sertel, and C. C. Chen, *Appl. Comput. Electrom.* **22**, 22 (2007).
- [29] S. Yarga, K. Sertel, and J. L. Volakis, *IEEE Trans. Antennas Propag.* **56**, 119 (2008).
- [30] S. Yarga, K. Sertel, and J. L. Volakis, *IEEE Antennas Wireless Propag. Lett.* **8**, 287 (2009).
- [31] S. Yarga, K. Sertel, and J. L. Volakis, *IEEE Trans. Antennas Propag.* **57**, 799 (2009).
- [32] Y. Cao, J. Schenk, T. J. Sulesk, M. A. Fiddy, J. Raquet, J. Ballato, K. Burbank, M. Graham, and P. Sanger, *Proc. SPIE* **6480**, 64800E (2007).
- [33] Y. Cao and M. A. Fiddy, *Proc. SPIE* **6128**, 61281I (2006).
- [34] A. V. Kanaev, Y. Cao, and M. A. Fiddy, *Opt. Eng.* **44**, 095201 (2005).
- [35] Y. Cao, J. Schenk, R. P. Ingel, M. A. Fiddy, K. Burbank, M. Graham, P. Sanger, and W. Yang, *Proc. SPIE* **6901**, 69010L (2008).
- [36] S. G. Johnson and J. D. Joannopoulos, *Opt. Express* **8**, 173 (2001).
- [37] H. Y. Ryu, M. Notomi, and Y. H. Lee, *Phys. Rev. B* **68**, 045209 (2003).